Ductile-Brittle Transition in Random Porous Au

Rong Li and K. Sieradzki

Department of Materials Science and Engineering, The Johns Hopkins University, Baltimore, Maryland 21218

(Received 12 July 1991)

We report experimental results describing the mechanical breakdown of random porous Au which is a new material specifically developed for this study. Digital image analysis was used to characterize the microstructures of the samples which varied by more than 2 orders of magnitude in length scale. The porous Au undergoes a microstructurally controlled ductile-brittle transition. Similar transitions have been found in numerical simulations by Kahng *et al.* [Phys. Rev. B **37**, 7625 (1988)].

PACS numbers: 62.20.Mk

Mechanical breakdown or fracture in random porous media has been the subject of considerable computational and theoretical research in recent years [1]. While there has been significant progress on these fronts [2–11] experimental results have not been quick to emerge. A small amount of experimental work in 2D has been done on diluted networklike systems using metal sheets with randomly positioned holes or "cracks" [12–14]. We know of no experimental work reported on disordered solids containing ligaments with a distribution of fracture strengths.

In this Letter, we report the first results on the fracture properties of a well characterized 3D random porous solid. The solid chosen for this study is new and has been specifically developed for this work. The material is highly porous Au which we believe should serve as a new model system for studying various physical properties associated with 3D random porous structures. The morphology of the porous Au shown in Fig. 1 is that of an interpenetrating solid-void composite similar to the structure of porous Vycor. As described below, this structure is produced from a single-phase Ag-Au alloy by selectively leaching out the Ag using an electrochemical process. Sieradzki *et al.* have studied the formation of these porous structures using computer simulation [15]. Porous metallic structures such as these can arise naturally during some alloy corrosion processes and are believed to lead to the phenomenon of stress-corrosion cracking [16,17] and alloy passivation [18]. The porous metallic materials introduced here have controllable microstructures spanning a range of ~ 2.5 orders of magnitude in size scale and should have great utility in phenomena dealing with random porous solids such as permeability, conductivity, elastic wave propagation [19], and light scattering [20].

One of the most interesting predictions to emerge from

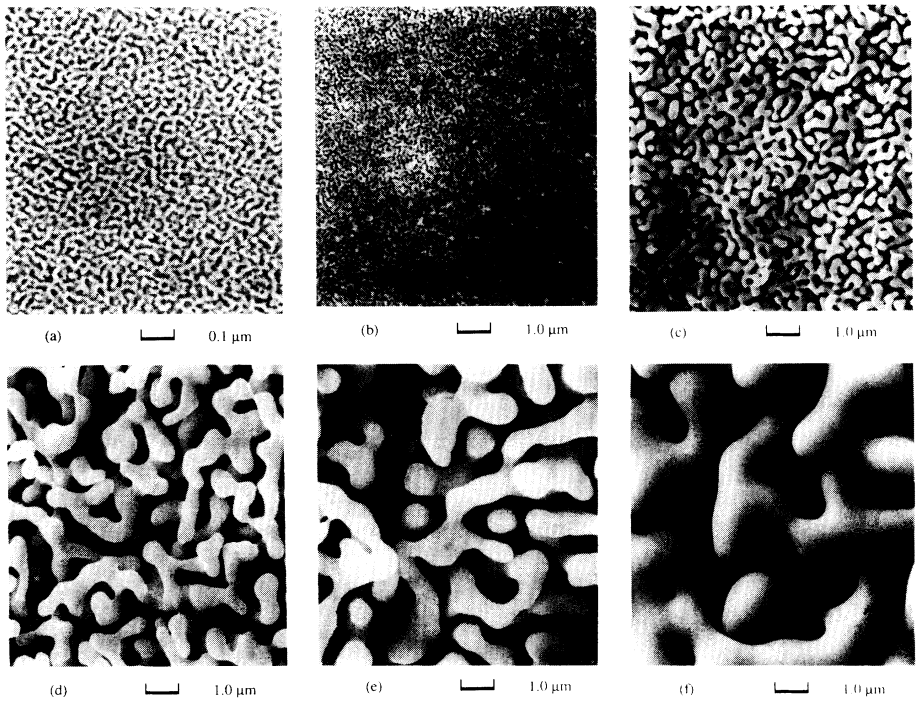

FIG. 1. Scanning electron micrographs showing the interpenetrating solid-void composite structure of the porous Au. The dealloyed samples were annealed at the indicated temperature for 10 min. (a) 100 °C, (b) 300 °C, (c) 500 °C, (d) 600 °C, (e) 700 °C, and (f) 800 °C. The magnifications of micrographs (b)–(f) are identical. Note that all samples have 24% of the density of bulk Au.

theory and computer modeling of fracture in disordered media is the prediction of a sample-size-dependent ductile-brittle transition. Kahng *et al.* [6] have presented a fracture map for the ductile-brittle behavior of a disordered network as a function of the distribution of element strengths and the sample size. In network systems the terms ductile and brittle refer to the nature of the damage introduced into the sample during the fracture process. If many separated or distributed microcracks develop in the sample during fracture, the behavior of the system is termed "ductile" and if only a few cracks form in the sample prior to failure, it is characterized as "brittle." This is quantified by defining an order parameter [6, 11,21,22], $n_b = N_b/L^{d-1}$, where N_b is the number of broken bonds or cracks and L is the sample size. For brittle fracture, $n_b \sim$ const, and for ductile fracture, $n_b \sim L^y$, where y is between 0 and 1 in 2D [6]. In our experiment the parameter N_b cannot be directly measured and we use the terms ductile and brittle in the more conventional sense, i.e., as a qualitative description of the magnitude of the fracture strain. The fracture strain, e_f, or the ductility is usually defined as δ_f/L, where δ_f is the extension at failure [23].

The porous gold samples described here were made from Ag-Au alloys containing 76 at.% Ag. The phase diagram for this binary alloy system displays perfect solid solubility across the entire range of compositions. The alloy was made by placing appropriate quantities of the constituent elements into a quartz tube which was evacuated, backfilled with an inert gas, and sealed. The quartz tube containing the Ag-Au mixture was placed in a furnace at 1100 °C for 1 h forming a cast ingot which was subsequently given a 900 °C homogenization treatment for 200 h. The homogeneity and composition of the ingot was confirmed by energy dispersive x-ray microprobe analysis [24]. Samples in the shape of approximately 2 mm × 2 mm × 30 mm beams were cut from the ingot and annealed at 900 °C for 24 h to relieve any residual stresses that may have developed during cutting operations.

The $Ag_{0.76}Au_{0.24}$ beams were placed in 1 M $HClO_4$ acid under an applied electrochemical potential of 1 V versus a standard calomel reference electrode for 12 h. This procedure results in the selective removal of Ag from the alloy and the concomitant formation of the interpenetrating void-Au structure with a size scale of ~3 nm [25]. Following dealloying each of the porous Au beams was given a coarsening treatment for 10 min at a prescribed temperature in the range of 100–800 °C. Figure 1 shows the spectacular microstructures obtained. There is more than 2 orders of magnitude spread in the length scales of the microstructures shown. Energy dispersive x-ray analysis was used to examine the composition of the porous Au beams following the coarsening treatment and showed that each of the samples contained trace amounts of Ag. The residual Ag develops owing to entrapment and is an expected consequence of the selective dissolution process [15].

Digital image analysis of the samples was performed using a scanning electron microscope in order to obtain a statistical characterization of the microstructures in the samples [26]. Histograms obtained for each sample were normalized to the largest value of the ordinate and abscissa found in that distribution and Fig. 2 displays the void-size histogram. A similar result was obtained for the ligament-size histogram. Since the failure stress or strain of the individual ligaments scales with the ligament size, these histograms provide us with a good description of the distribution of element strengths which characterize these solids. There is a slight tendency for an increase in the width of the distributions with increasing annealing temperature, and this is an expected result of the coarsening process.

Load-displacement (P-δ) curves to fracture were obtained for each of the samples in three-point bending, under displacement control. The P-δ curves allowed us to obtain the fracture load, P_f (and stress σ_f), the load-point displacement at fracture, δ_f, and the fracture energy or the toughness, W. The P-δ curves for the samples annealed at 100 and 300 °C were linear to sample failure, whereas the curves for the other samples displayed mild curvature (concave downward) which increased with increasing annealing temperature. For all the samples examined, instability and sample fracture occurred at the maximum load. Figure 3 shows the results obtained for P_f, δ_f, and W plotted against the parameter N/A, the number of voids per unit area (1 μm^2). The fracture energy which varies by a factor of 60 for the samples investigated is a conventional indicator of a fracture mode

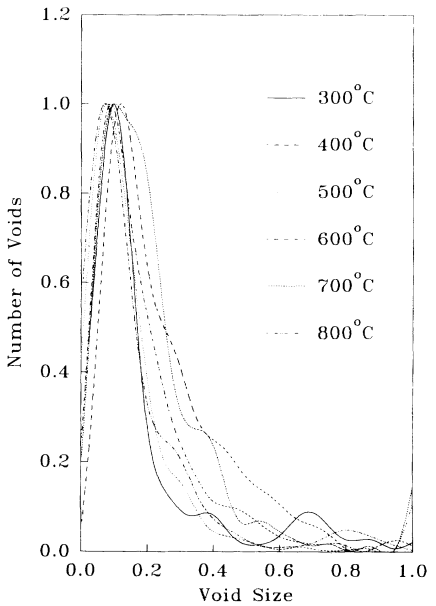

FIG. 2. The normalized void-size histograms of the porous Au samples formed from the $Ag_{0.76}Au_{0.24}$ alloy. Digital image analysis could not be performed for the sample annealed at 100 °C owing to the size scale of the microstructure obtained.

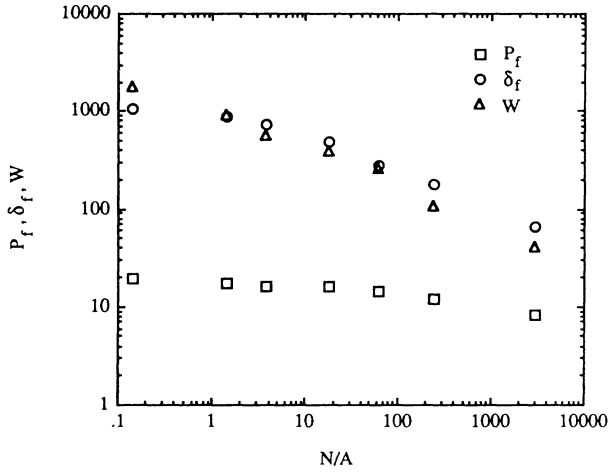

FIG. 3. Experimental data for the fracture load, P_f ($kg \times 10^{-3}$), load point displacement at fracture, δ_f (μm), and fracture energy, W ($J \times 10^{-7}$), plotted against the parameter N/A for the porous Au samples investigated. N/A is the number of pores in 1 μm^2 of sample area.

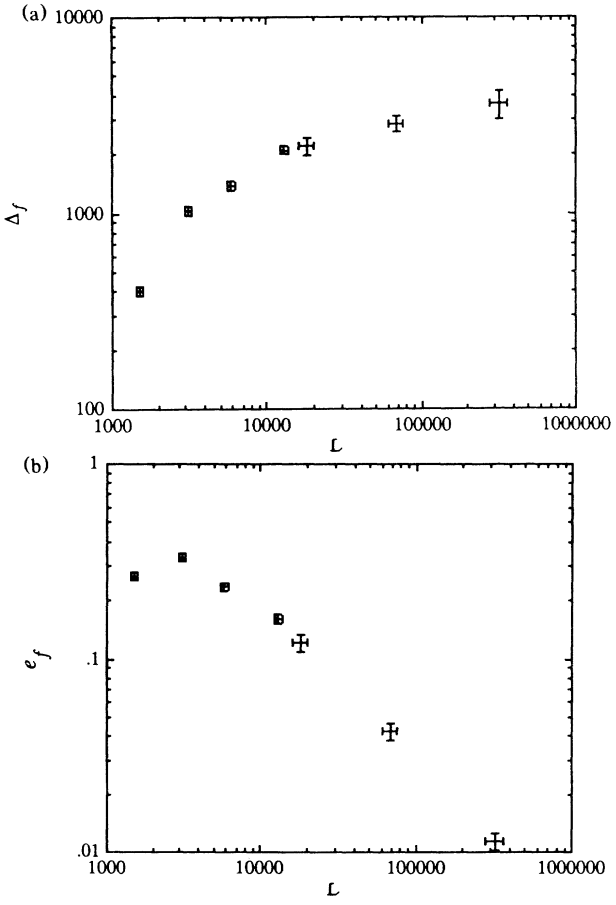

FIG. 4. (a) Scaled fracture displacement Δ_f and (b) fracture strain e_f vs the scaled sample size $\mathcal{L}$, where $\Delta_f = \delta_f/(A/N)^{0.5}$, $\mathcal{L} = L(A/N)^{0.5}$, and $e_f = \Delta_f/\mathcal{L}$. If we assume that all failed ligaments contribute equally to δ_f, then Δ_f can be considered as a measure of the number of broken ligaments at failure.

transition.

A convenient way of analyzing the test results is to use the nature length scale in each of the structures as a normalization parameter. This allows for a more straightforward comparison of our experimental results with analytical and simulation work of other investigators. We use the average cell size, $(A/N)^{1/2}$, as this parameter and scale physical parameters accordingly. The results are plotted against a parameter $\mathcal{L} = L/(A/N)^{1/2}$ (where L is the width of the beam in μm) which may be considered to be a measure of the sample size in units corresponding to the natural length scale of each structure. Figure 4 shows the behavior of the normalized parameters Δ_f and e_f as a function of $\mathcal{L}$. This figure demonstrates that there are two distinct regions of behavior. For small $\mathcal{L}$, $\Delta_f \sim \mathcal{L}^b$, with $b \cong 0.75$, and as $\mathcal{L}$ increases, Δ_f saturates and becomes weakly dependent on $\mathcal{L}$. The fracture strains at small $\mathcal{L}$ are large and indicative of ductile behavior whereas the fracture strains for large $\mathcal{L}$ are approaching values more typical of brittle behavior. Figure 5 shows that the behavior of the fracture stress, σ_f, is unclear as we cannot distinguish between power-law decay of σ_f with $\mathcal{L}$ or behavior of the form $1/(\ln \mathcal{L})^y$. Similar ambiguities have been reported in numerical simulations [6].

Our treatment of the data assumes that there is no microscopic ductile-brittle transition that occurs in the failure mechanism with increasing sample size. For example, deformation and fracture in metals is often related to dislocation density. The initial dislocation density of the alloy is low enough ($\sim 10^6$ cm^{-2}) so that the samples

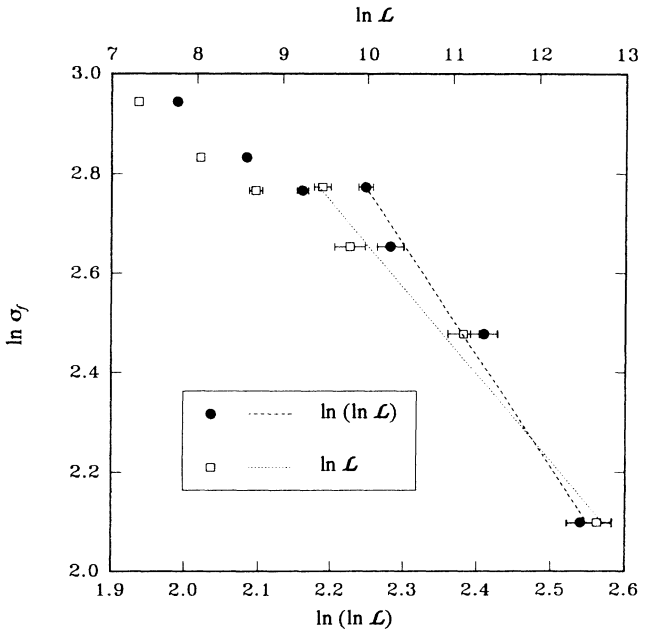

FIG. 5. The fracture stress σ_f is plotted vs $\mathcal{L}$ and $\ln \mathcal{L}$, respectively, on a double logarithmic scale. By successively deleting the smaller L points we determined that for $\sigma_f \sim \mathcal{L}^{-b}$, $b \cong 0.2$, and for $\sigma_f \sim (\ln \mathcal{L})^{-y}$, $y \cong 2.2$.

containing ligaments of the order of 10 nm in diameter should contain few (if any) grown in dislocations compared to the samples with 1000-nm-diam ligaments. We believe that issues such as this should have negligible effect on the behavior of our samples because surface dislocation sources would be expected to swamp out effects resulting from such variations [27,28]. These arguments are supported by our microscopic examination of the failed samples. High-resolution scanning electron microscopy of the fractured ligaments of the failed samples showed that all the samples had ligaments displaying both slanted and flat fracture faces. The general phenomenology which we observed for ligament fracture in porous gold is consistent with results of earlier studies on fracture of microscopic gold crystals conducted by Wilsdorf [28]. Our investigation does not support the possibility that the ductile-brittle transition which we observe is microscopic in origin.

In summary, we have presented experimental results for mechanical failure in random porous gold structures. We observe a microstructural length scale controlled ductile-brittle transition in these structures which is similar to previous results for a network system described by Kahng *et al.* [6]. Let us note that our system is more complicated than the elastic systems studied numerically by previous investigators in that the ligaments comprising the porous gold display elastic-plastic behavior. Our results indicate that the sample-size-driven ductile-brittle transition may be quite universal with respect to the exact nature of the constitutive behavior of the individual ligaments in the random structure.

We are grateful for the support of the U.S. Department of Energy, Division of Materials Sciences, Office of Basic Energy Sciences under Contract No. DE-FG02-90ER45421.

[1] See, for example, *Statistical Models for the Fracture of Disordered Media,* edited by H. J. Herrmann and S. Roux (North-Holland, Amsterdam, 1990).

[2] P. M. Duxbury, P. D. Beale, and P. L. Leath, Phys. Rev. Lett. **57**, 1052 (1986).

[3] P. M. Duxbury, P. L. Leath, and P. D. Beale, Phys. Rev. B **36**, 367 (1987).

[4] A. Hansen, E. L. Hinrichsen, and S. Roux, Phys. Rev. Lett. **66**, 2476 (1991).

[5] P. D. Beale and D. J. Srolovitz, Phys. Rev. B **37**, 5500 (1988).

[6] B. Kahng, G. G. Barttrouni, S. Redner, L. de Archangelis, and H. J. Herrmann, Phys. Rev. B **37**, 7625 (1988).

[7] D. Sornette, J. Phys. (Paris) **50**, 745 (1989).

[8] A. Gilbert, M. Benayad, A. Sornette, D. Sornette, and C. Vanneste, J. Phys. (Paris) **51**, 33 (1990).

[9] M. D. Stephens and M. Sahimi, Phys. Rev. A **36**, 8656 (1987).

[10] B. K. Chakrabarti, D. Chowdhury, and D. Stauffer, Z. Phys. B **62**, 343 (1986).

[11] H. J. Hermann, A. Hansen, and S. Roux, Phys. Rev. B **39**, 637 (1989).

[12] K. Sieradzki and R. Li, Phys. Rev. Lett. **56**, 2509 (1986).

[13] L. Benguigi, P. Ron, and D. J. Bergmann, J. Phys. (Paris) **48**, 1547 (1987).

[14] Rong Li, Ph.D. dissertation, Queens College, CUNY, 1989 (unpublished).

[15] K. Sieradzki, R. R. Corderman, K. Shukla, and R. C. Newman, Philos. Mag. **59**, 713 (1989).

[16] K. Sieradzki and R. C. Newman, J. Phys. Chem. Solids **48**, 1101 (1987).

[17] R. G. Kelly, A. J. Frost, T. Shahrabi, and R. C. Newman, Metall. Trans. (to be published).

[18] Q. Song, R. C. Newman, R. A. Cottis, and K. Sieradzki, J. Electrochem. Soc. **137**, 435 (1990).

[19] See, for example, C. W. Kiewiet, H. E. Hall, and J. D. Reppy, Phys. Rev. Lett. **35**, 1286 (1975); D. S. Fisher and M. P. A. Fisher, Phys. Rev. Lett. **61**, 1847 (1988).

[20] M. Bishop, K. Langley, and F. Karasz, Phys. Rev. Lett. **57**, 1741 (1986).

[21] P. M. Duxburry and S. G. Kim, in *Mechanical Properties of Porous and Cellular Materials,* edited by K. Sieradzki, D. Green, and L. J. Gibson, MRS Symposia Proceedings No. 207 (Materials Research Society, Pittsburgh, PA, 1991), p. 179.

[22] Y. S. Li and P. M. Duxburry, Phys. Rev. B **38**, 9527 (1988).

[23] For large e the fracture strain or "ductility" is actually defined as $\varepsilon_f = \ln(1+e_f)$ and is referred to in terms of the true strain. For our purposes it is not necessary to make this distinction. See, for example, G. Dieter, *Mechanical Metallurgy* (McGraw-Hill, New York, 1986), 3rd ed.

[24] The Ag content was determined using elemental and alloy standards with the program FUNDAMENTAL PARAMETERS (Tracor Northern, Princeton, NJ).

[25] The 3-nm pore size is too small to be observed with the technique used to characterize the other samples, i.e., high-resolution scanning electron microscopy. Instead we used scanning tunneling microscopy and transmission electron microscopy to examine the as dealloyed samples. No digital image analysis was performed on these structures and the 3-nm dimension is represents an average of only a few measurements.

[26] The digital image analysis was performed using the Tracor Northern model 5500 x-ray analysis system which incorporates the routine VISTA (Tracor Northern, Princeton, NJ).

[27] J. P. Hirth, *Relation between Structure and Strength in Metals and Alloys* (H. M. Stationary Office, London, 1963), p. 218.

[28] H. G. F. Wilsdorf, Acta Metall. **30**, 1247 (1982).

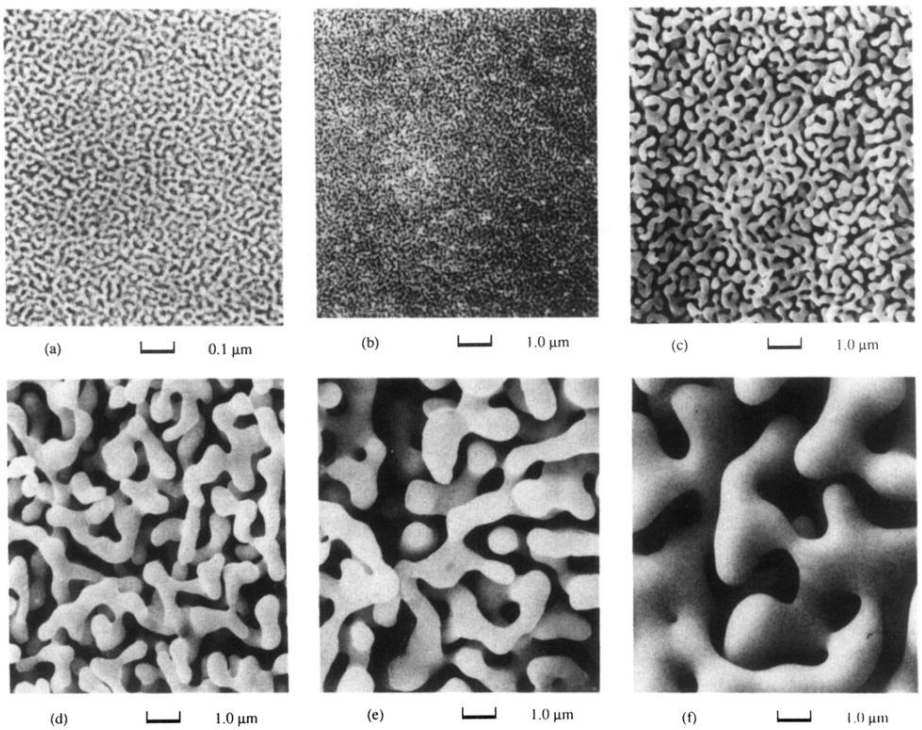

FIG. 1. Scanning electron micrographs showing the interpenetrating solid-void composite structure of the porous Au. The dealloyed samples were annealed at the indicated temperature for 10 min. (a) 100 °C, (b) 300 °C, (c) 500 °C, (d) 600 °C, (e) 700 °C, and (f) 800 °C. The magnifications of micrographs (b)–(f) are identical. Note that all samples have 24% of the density of bulk Au.